Dithienocoronenediimide-Based Copolymers as Novel Ambipolar Semiconductors for Organic Thin-Film Transistors

ARTICLE *in* ADVANCED MATERIALS · JULY 2012

Impact Factor: 17.49 · DOI: 10.1002/adma.201201014 · Source: PubMed

4 AUTHORS, INCLUDING:

Hakan Usta
Abdullah Gül Üniversitesi
38 PUBLICATIONS **1,636** CITATIONS
SEE PROFILE

Antonio Facchetti
Northwestern University
381 PUBLICATIONS **22,191** CITATIONS
SEE PROFILE

ADVANCED MATERIALS
www.advmat.de

www.MaterialsViews.com

Dithienocoronenediimide-Based Copolymers as Novel Ambipolar Semiconductors for Organic Thin-Film Transistors

Hakan Usta, Christopher Newman, Zhihua Chen, and Antonio Facchetti**

Solution processible π-conjugated polymers are of extensive scientific and technological interest as semiconducting materials in organic electronics.[1] Compared to small molecules, tuned rheological properties of polymeric solutions enable proper ink formulations for high-throughput printing processes on large-area, light-weight, and flexible substrates.[2] Since the demonstration of the first polymeric semiconductor based on a electrochemically grown polythiophene,[3a] a number of semiconducting polymers with a wide range of optoelectronic properties have emerged, which has been crucial for developing high-performance organic thin-film transistors (OTFTs), light-emitting transistors (OLETs), and photovoltaic cells (OPVs), as well as to better understanding charge transport mechanisms.[3] Today, the majority of the state-of-the-art semiconducting polymers are unipolar -i.e., either *p*-type (hole-transporting) or *n*-type (electron-transporting) - and they exhibit air-stable charge carrier mobilities reliably exceeding that of amorphous silicon (~0.1 $cm^2 V^{-1} s^{-1}$) and even reaching commercially-relevant values (~0.5–1.0 $cm^2 V^{-1} s^{-1}$).[4,5] Additionally, bulk heterojunction OPVs having π-conjugated polymers with either the donor or the acceptor unit have now enabled power conversion efficiencies of >7%.[6] Among several optoelectronic applications of π-conjugated polymers, there are relatively few examples of low band-gap ambipolar polymers, and typical electron/hole mobilities are ~0.01–0.1 $cm^2 V^{-1} s^{-1}$ under nitrogen.[7] Only recently, after careful optimization of polymer structure, device architecture, charge injection, and processing conditions, high hole/electron mobilities of ~0.3–1.0 $cm^2 V^{-1} s^{-1}$ were achieved under nitrogen.[8] Nevertheless, very few single-component ambipolar polymers are known to operate in ambient, and they generally exhibit modest hole/electron mobilities (~10^{-4}–10^{-3} $cm^2 V^{-1} s^{-1}$).[9] Realizing solution-processable ambipolar polymers which operate in ambient is very important for the further development of single-component CMOS-type organic logic circuits and light emitting transistors (OLETs), as well as fundamental understanding of electron vs. hole transport in polymer solids.[10]

The common approach to achieve ambipolarity in polymers relies on the construction of strong donor-acceptor (D-A) backbones with alternating π-electron deficient (acceptor) and π-electron rich (donor) conjugated moieties. This strategy yields low band-gap electronic structures, where both the highest occupied molecular orbital (HOMO) and lowest unoccupied molecular orbital (LUMO) are within the injection regime of the source/drain electrodes, and low- and high-energy enough to minimize severe charge trapping. Furthermore, in this architecture both type of charge carriers can be effectively transported in the solid state via donor/acceptor π-orbital intrachain delocalization and interchain overlap. From a synthetic standpoint, one of the main challenges hampering the development of new high-performance ambipolar polymers is the design and synthesis of new polymerizable π-electron deficient acceptors with good charge-transporting properties. Therefore, the current ambipolar polymers with appreciable charge carrier mobilities (>0.01 $cm^2 V^{-1} s^{-1}$) span only a limited range of acceptor units such as diketopyrrolopyrrole (DPP), benzo(bis) thiadiazole (BTZ), and naphthalenediimide (NDI).[7,8] Among these, π-conjugated diimides have rarely been explored as an acceptor unit, although their small molecule derivatives ranging from pyromellitic diimides to quaterrylene diimides have showed great promise in *n*-channel OTFTs.[11,12] Additionally, a semiconductor based on coronenediimide (CDI) core has yet to be reported in OTFTs, which is rather surprising since the coronene core has a highly planar, rigid and extended aromatic system with a perfect delocalization of aromaticity in a six fold symmetry.[13] Indeed, to the best of our knowledge, the only reports of charge carrier mobilities on coronene(di) imides were observed by space charge limited current (SCLC) or microwave conductivity (PR-TRMC) techniques, and their poor FET performances have been attributed to the unfavorable microstructure with a face-on orientation on the surface.[14] The above considerations and the possibility that incorporation of highly extended, π-electron deficient coronenediimides into low band gap polymeric backbones might facilitate efficient hole/electron transport prompted us to investigate new polymers as potential ambipolar semiconductors for OTFTs.

In this paper, we report three novel polymers P1–P3 embedding a dithienocoronenediimide (DTCDI) acceptor unit along with thiophene, bithiophene, and 3,3'-dialkoxybithiophene donor moieties (**Scheme 1**). Top-gate bottom-contact (TG-BC) TFTs are fabricated by spin-coating two of these polymers solutions, and they exhibit ambipolar behavior in ambient with electron and hole mobilities of up to 0.30 $cm^2 V^{-1} s^{-1}$ and 0.04 $cm^2 V^{-1} s^{-1}$, respectively. Devices exhibit negligible variations in TFT characteristics when stored in ambient for one week. To the best of our knowledge, these mobilities are the highest reported to date in ambient for an ambipolar polymer in a top-gate/bottom-contact architecture. Furthermore, P1 and

Dr. H. Usta, Dr. C. Newman, Dr. Z. Chen,
Prof. A. Facchetti
Polyera Corporation, 8045 Lamon Ave. Skokie
IL 60077, USA
E-mail: husta@polyera.com; afacchetti@polyera.com

DOI: 10.1002/adma.201201014

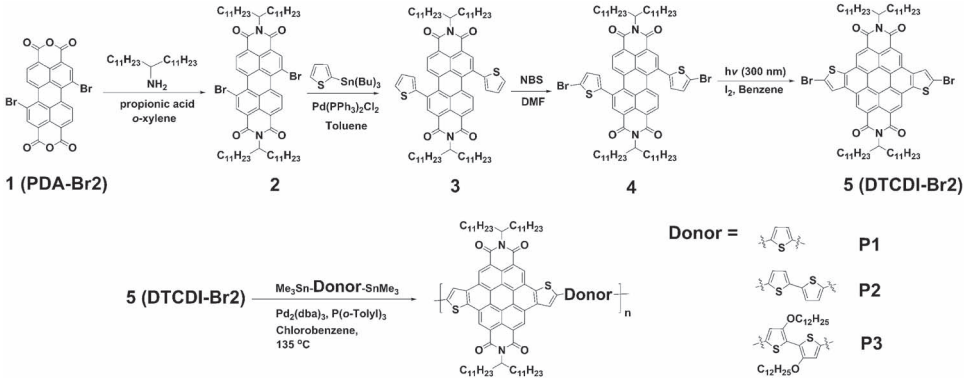

Scheme 1. Synthetic route to monomer 5(DTCDI-Br2) and polymers P1-P3.

P3 are the first examples of coronenediimide-based semiconductors showing high OTFT performances.

The new core was synthesized via a very high-yield photocyclization reaction and has a strong tendency to form π–π stacks (vide infra).[15] Based on pre-synthesis computational modeling, DTCDI-thiophene copolymers should have an highly coplanar backbone (**Figure 1**). This is a significant advantage versus PDI- and NDI-based systems, where the existence of six-five inter-ring linkages and sterically encumbered bay region (in the perylenediimide case) causes significant polymer backbone torsion (~45–70°, Figure 1).[16] Additionally, DTCDI exhibits a linear monomer-linkage geometry with negligible angle difference between *syn*- and *anti*- regioisomers, whereas previously reported PDI-based copolymers having *1,6* and *1,7* regioisomers include two completely different backbone architectures - zigzag vs. linear (Figure 1). This is very critical to achieve a high degree of regioregularity in a polymeric backbone, which is known to be crucial for OTFT device performance.[17]

Scheme 1 shows the synthesis of dithienocoronenediimide building block DTCDI-Br2 (5) and the corresponding copolymers P1–P3. Note that the starting material 1 (PDA-Br2) is a mixture of 1,6- and 1,7-regioisomers; however, for simplicity,

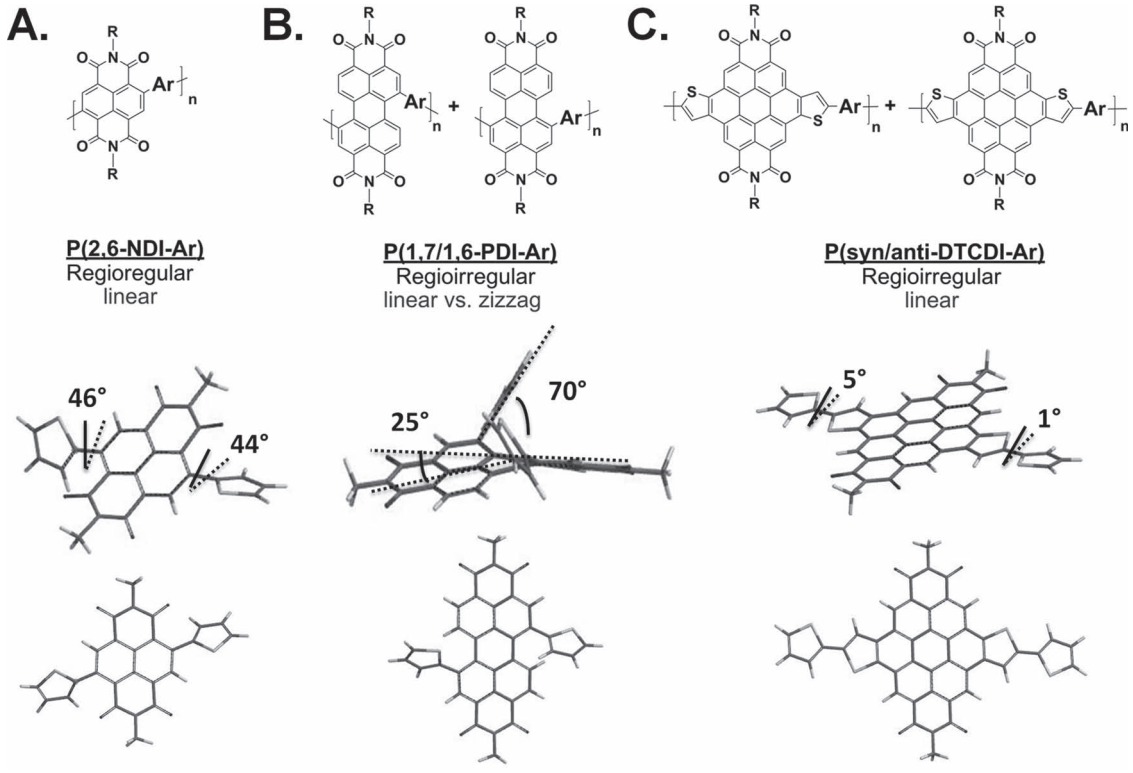

Figure 1. Chemical structures and DFT-calculated molecular geometries of naphthalenediimide (NDI)- (A), perylenediimide (PDI)- (B), and dithienocoronenediimide (DTCDI)-based (C) copolymers illustrating dihedral angles and the effect of regioregularity on the polymer backbone architecture (B3LYP/6-31G** level of theory).

only the 1,7-regioisomer is shown here. Although previous research demonstrated that regioisomerically pure 1,7-disubstituted PDIs can be obtained with some specific imide/bay substitutions via repetitive crystallizations, the method is cumbersome and works only with specific substituents.[18] Therefore, most of the previously reported PDI-based semiconductors are a mixture of regioisomers.[19,20] 1,7(1,6)-Dibromoperylenedianhydride (1) was converted to compound 2 via an imidization reaction with 12-tricosanamine in propionic acid/*o*-xylene in 36% yield. The low reaction yield is attributed to nucleophilic displacement of the bromine atoms by secondary 12-tricosanamine resulting in core-substituted amine by-products. Compound 2 was coupled with 2-(tributylstannyl)thiophene via a Stille reaction using $Pd(PPh_3)_2Cl_2$/toluene as the catalyst/solvent system to give compound 3 in 87% yield. Despite the extension of the π-conjugation upon thiophene substitution, 3 was found to be more soluble than 2. This is probably due to poor π–π stacking interactions between distorted PDI cores caused by the presence of thiophene groups in the bay region (Figure 1). α-Bromination of compound 3 with NBS in DMF yields compound 4 (70% yield), which undergoes a facile photocyclization reaction (λ = 300 nm) in the presence of I_2 to afford the monomer 5 in quantitative yields (98%). Compounds 2–5 were characterized by ^{1}H NMR, ^{13}C NMR, Elemental Analysis, and Mass Spectroscopy (MALDI-TOF). It's noteworthy that when compounds 3 and 4 are stored as dilute solutions ($<10^{-3}$ M) in air under normal lab lighting, the DTCDI core forms in several hours, indicating a highly favorable photocyclization-probably using ambient O_2 as the oxidant. Interestingly, ^{1}H NMR spectra of monomer 5 was found to be concentration dependent. Therefore, we synthesized a model compound T-DTCDI-T in order to mimic a polymeric backbone with thiophene moieties and to eliminate the effect of bromine substituents (Scheme S1). Concentration-dependent ^{1}H NMR analysis of this model compound shows that the protons assigned to the aromatic core shift upfield with increasing concentration (δ = 7.56–9.78 ppm → 7.10–9.24 ppm), indicating a shielding effect caused by staggered π–π stacking between T-DTCDI-T molecules (Figure S1).[21] Additionally, the distribution of the aromatic-core proton resonances becomes wider with increasing the concentration (0.15–0.30 ppm → 0.50–0.60 ppm), indicating a greater number of local electronic enviroments, which further supports this stacking model.[21c] Similar stacking characteristics have been observed in the literature for a number of disc-like hexabenzocoronene-based compounds, and it's crucial to efficient charger-carrier transport in various applications.[22]

The copolymers P1–P3 were synthesized via conventional Stille polycondensation protocols by reacting the monomer 5 with 2,5-bis(trimethyltin)thiophene, 5,5′-bis(trimethyltin)-2,2′-bithiophene, and 5,5′- bis(trimethylstannyl)-3,3′-didodecyloxy-2,2′-bithiophene, respectively in chlorobenzene using $Pd_2(dba)_3$/P(*o*-tolyl)$_3$ as the catalyst/ligand system. Although P1 and P3 were highly soluble in common organic solvents, P2 is insoluble preventing further purification and characterization. P1 and P3 were purified by sequential soxhlet extractions and multiple dissolution-precipitation processes (85–97% yields). Polymer molecular weights determined by GPC versus polystyrene indicate number-average molecular weights (M_n) of 11K Da (PDI = 1.6) for P1 and 51K Da (PDI = 1.7) for P3.

The optical absorption spectra and cyclic voltammograms of thin-films of DTCDI building block 5 and polymers P1 and P3 are shown in **Figure 2**, and data are collected in **Table 1**. Compound 5 exhibits two main absorptions with λ_{max} located

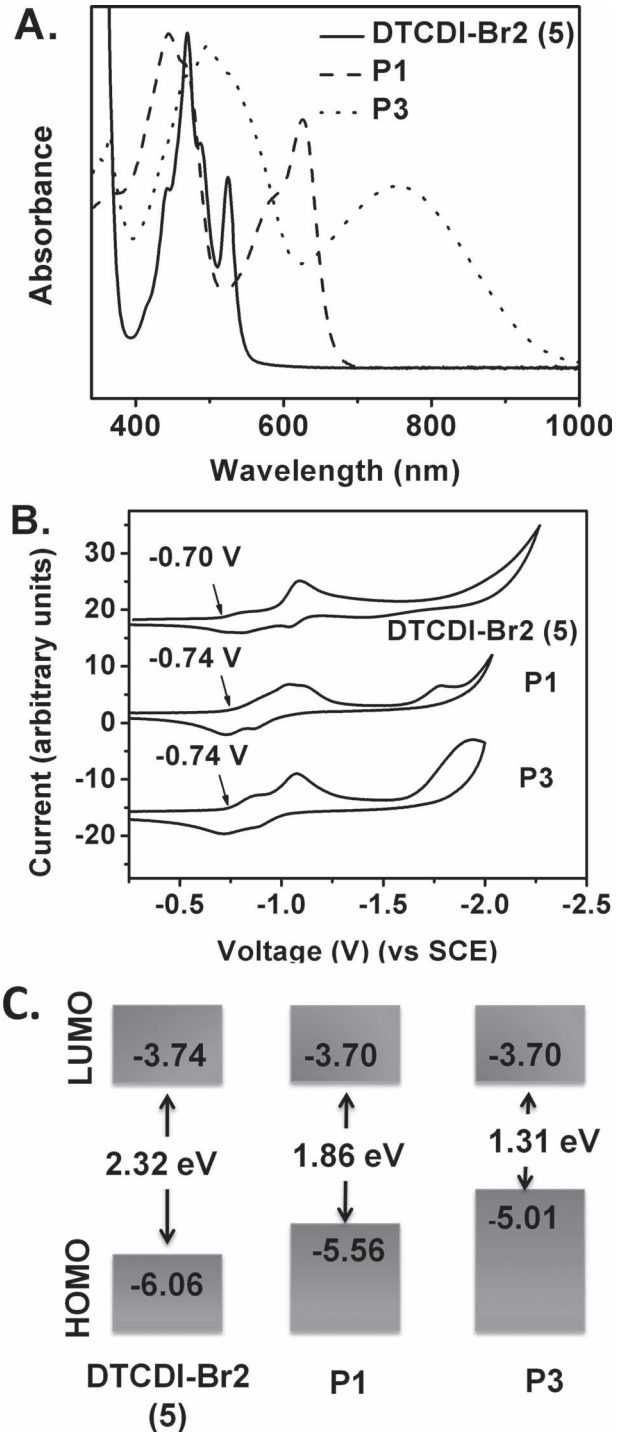

Figure 2. (A) UV-vis absorption spectra of spin-coated films of 5, P1, and P3 on glass. (B) Cyclic voltammograms of 5, P1, and P3 as thin films in 0.1 M $Bu_4N^+PF_6^-$ solution in acetonitrile at a scan rate of 100 mV/s. (C) The energy diagram for 5, P1, and P3 showing experimentally estimated HOMO/LUMO energy levels.

Table 1. Summary of Optical Absorption,[a] Electrochemical Properties,[b] Molecular Weights,[c] and Field-Effect Mobilities, Current on/off Ratios, and Threshold Voltages,[d] of Compounds DTCDI-Br2 (5), P1, and P3, and Corresponding Estimated Frontier Molecular Orbital Energies.[e]

Compd.	M_n [kDa]	PDI	E_{red1} [V]	LUMO [eV]	HOMO [eV]	λ_{abs}[nm] (E_g [eV])	μ_{avg} [$cm^2V^{-1}s^{-1}$]	μ_{max} [eV]	I_{on}/I_{off}	V_T [V]
5	N/A	N/A	–0.70	–3.74	–6.06	469*,526(2.32)	N/A	N/A	N/A	N/A
P1	10.7	1.6	–0.74	–3.70	–5.56	444*,625(1.86)	0.1–0.2 (e^-)	0.30	5–6	+34
							0.008–0.01 (h^+)	0.04	4–5	–41
P3	51.0	1.7	–0.74	–3.70	–5.01	498*,755(1.31)	0.01–0.02 (e^-)	0.03	5–6	+47
							0.001–0.002 (h^+)	0.003	3–4	–65

[a]As spin-coated thin film on glass, optical band gap is estimated from the low-energy band edge of the UV-vis spectrum; [b]As thin-film on Pt electrode in 0.1 M $TBAPF_6$/Acetonitrile vs. SCE; [c]Room temperature gel-permeation chromatography (GPC) in THF vs. PS standards; [d]Field-effect carrier mobilities and current on/off ratios for holes (h^+) and electrons (e^-) calculated in the saturation regime for top-gate bottom-contact TFT architecture with substrate (glass)/Au (source-drain electrodes)/semiconductor(P1 or P3)/polymeric dielectric (PMMA)/Au(gate contact); [e]Estimated vs. vacuum level from $E_{LUMO} = -4.44$ eV$-E_{red1}$ and $E_{HOMO} = E_{LUMO}-E_g$.

at 469 nm, indicating a significant hypsochromic shift of ~102 nm relative to the acyclic precursor 4 (λ_{max} = 571 nm, Figure S2). The corresponding optical band gap for 5 is estimated as 2.32 eV, which is ~0.4 eV higher than that of 4 (E_g^{opt} = 1.95 eV). Additionally, in contrast to the broad absorption bands observed for 4, the DTCDI core exhibits well-defined vibronic features, similar to non-substituted PDIs. These changes as a whole are indicative of enhanced π-conjugation along the short molecular axis and improved planarity/rigidity of the molecular backbone upon photocyclization, which is consistent with previous theoretical and experimental reports.[14a,23] The thin film polymer optical absorption spectra exhibits two/three main absorptions located at λ_{max} = 444/625 nm for P1 and λ_{max} = 498/755 nm for P3 and the corresponding optical band gaps are 1.86 eV and 1.31 eV, respectively. From cyclic voltammetry measurements, 5, P1 and P3 thin-films exhibit multiple (quasi) reversible reductions with the onset potentials of –0.70 V, –0.74, and –0.74 V, respectively (Figure 2B). Based on solid-state optical and electrochemical data, the HOMO/LUMO energies are estimated as –6.06/–3.74 eV for 5, 5.56/–3.70 eV for P1, and –5.01/–3.70 eV for P3. The HOMO and LUMO energy levels of the new DTCDI core are ~0.3–0.4 eV higher than those of well-studied PDI cores,[16a] reflecting the effect of π-electron rich thiophene annulation to the bay region. Similar to previously reported donor-acceptor copolymers, while the LUMO of the present polymers primarily depends on the DTCDI acceptor unit, the HOMO energy level changes with the π-electron richness of the donor unit.[20,16b] The well-balanced HOMO/LUMO energy levels of P1 and P3, as a result of the observed low band-gaps–are expected to impart injection/transport of both types of charge carriers.

Top-gate bottom-contact OTFTs were fabricated with P1 and P3 as the semiconducting layer. This device architecture is preferred due to the superior injection characteristics of the staggered device geometry and to the encapsulation effect of the top dielectric layer for the underlying semiconductor.[24] Additionally, facile channel miniaturization is feasible with bottom-contact TFTs to enable high-frequency circuits.[4] The semiconductor thin-films (~40–50 nm) were deposited on untreated Au (S-D contacts)/glass substrates by spin-coating polymer solutions (~5–10 mg/mL in DCB). Next, the polymeric dielectric layer (PMMA in *n*-butylacetate) was spin-coated. The devices were annealed before depositing the Au gate electrode via thermal evaporation. All device processing and electrical measurements were performed in ambient except the Au contact vapor deposition and film drying steps (see Supplementary Information). Mobilities (μ) are calculated in the saturation regime by the equation: $\mu = (2I_{SD}L)/[WC_i(V_{SG} - V_{th})^2]$. The transfer plots are shown in **Figure 3**A–D, and the OTFT device characteristics are summarized in Table 1. Both P1 and P3 devices showed clear ambipolar characteristics. For P1, the average electron and hole mobilities are 0.1–0.2 $cm^2\ V^{-1}\ s^{-1}$ and 0.008–0.01 $cm^2\ V^{-1}\ s^{-1}$, respectively, with the maximum mobilities of 0.30 $cm^2\ V^{-1}\ s^{-1}$ (e^-) and 0.04 $cm^2\ V^{-1}\ s^{-1}$ (h^+). P3 exhibits lower average electron and hole mobilities of 0.01–0.02 $cm^2\ V^{-1}\ s^{-1}$ and 0.001–0.002 $cm^2\ V^{-1}\ s^{-1}$, respectively, with the maximum mobilities of 0.03 $cm^2/V\cdot s$ (e^-) and 0.003 $cm^2\ V^{-1}\ s^{-1}$ (h^+). The current on/off ratios are 10^5–10^6 (P1 and P3) for *n*-channel operations, and 10^4–10^5 (P1) and 10^3–10^4 (P3) for *p*-channel operations. The electron mobilities of P1 and P3 are >10× higher than those of structurally similar PDI-thiophene copolymers (μ_e = 0.001–0.01 $cm^2/V\cdot s$), which were previously measured both in top-gate/bottom-contact and bottom-gate/top-contact device configurations.[4,19b,20] This result suggests that in our current DTCDI-based polymer system charge transport becomes more efficient due to highly planar polymeric backbone and enhanced regioregularity, which may facilitate intrachain charge delocalization, interchain charge transport, and thin-film microstructure (vide infra). It is noteworthy that similar electron/hole mobilities are measured for P1 and P3 devices even after 1 week of storage in ambient (Figure S3), indicating negligible deterioration due to ambient trapping species (O_2/H_2O). It is most likely that the observed device stability is due to an interplay of polymer electronic structure, uniform film morphology (vide infra), and self-encapsulated top-gate TFT architecture. Note that although ambipolarity can be observed for donor-acceptor polymers with π-conjugated diimides, the maximum hole mobilities are usually much lower than the maximum electron mobilities ($\mu_{e,max}/\mu_{h,max}$ ~ 50–100), which is consistent with the previously reported naphthalenediimide-based ambipolar polymer, PNBIT ($\mu_{e,max}/\mu_{h,max}$ ~ 100).[12] This indicates that the electron transport is inherently more facile compared to the hole transport for these π-conjugated diimide-based copolymers.

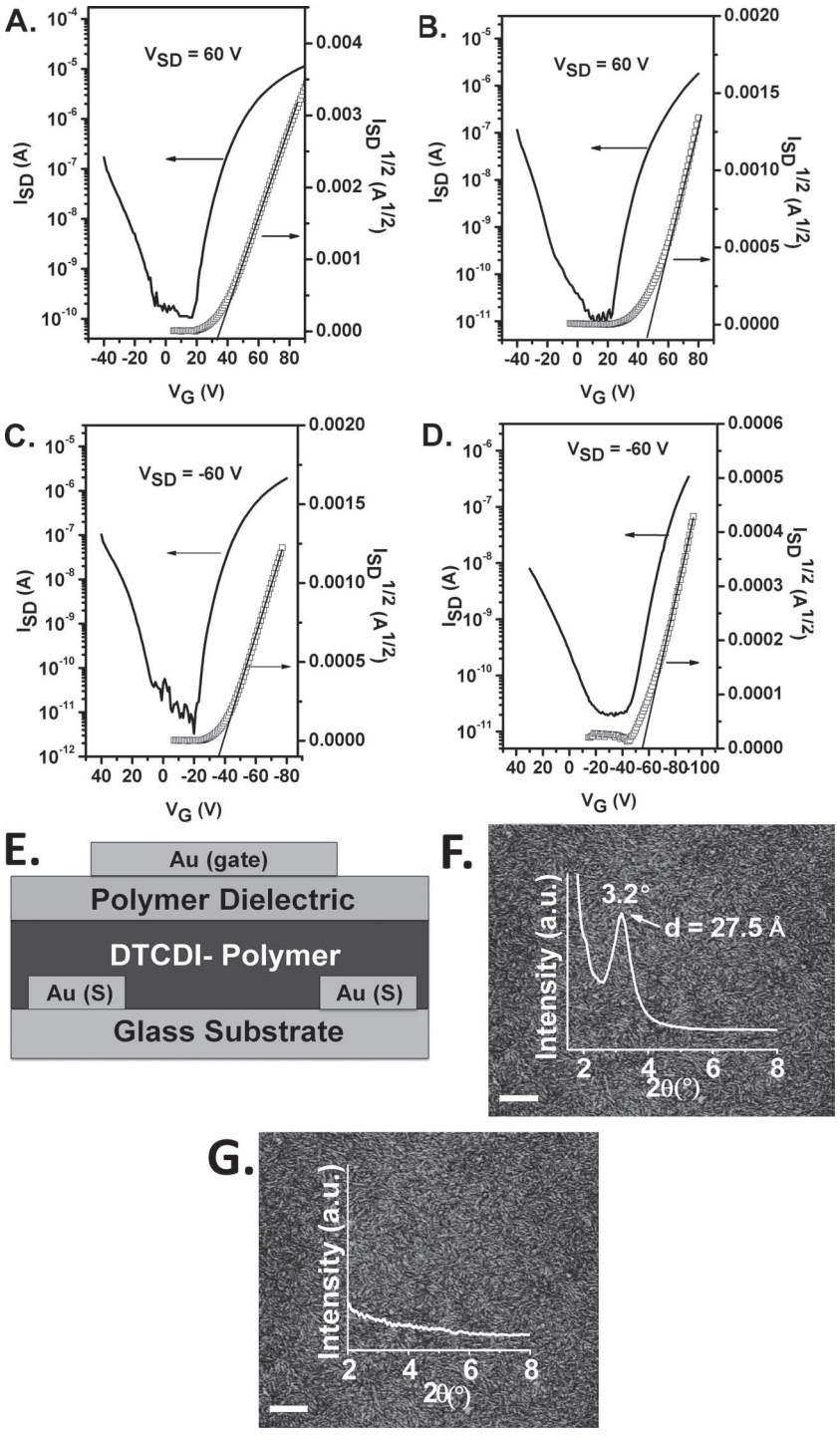

Figure 3. OTFT response plots of devices fabricated with P1 and P3. N-channel transfer plots of P1 (A) and P3 (B) at V_{SD} = 60 V in ambient. P-channel transfer plots of P1 (C) and P3 (D) at V_{SD} = –60 V in ambient. Top-gate/bottom-contact OTFT device structure (E), and tapping mode AFM images of spin-coated films of P1 (F) and P3 (G) with θ-2θ XRD scans (inset). Scale bars denote 1 μm.

Thin-film microstructures and morphologies of the present polymers were studied by θ-2θ X-ray diffraction (XRD) and atomic-force-microscopy (AFM). As shown in Figure 3F and G, AFM characterization of P1 and P3 thin-films reveals highly uniform and smooth (rms roughness of <3–4 nm for 10 μm × 10 μm scan area) surface morphologies, which are composed of tightly packed, highly interconnected, and well-defined nanofibers. The average width of these nanofibrous features are ~50–100 nm. The corresponding X-Ray diffraction (XRD) scans show that P1 films exhibit one first order Bragg reflection peak at 3.2°, while P3 films exhibit negligible reflections. This peak corresponds to an out-of-plane d-spacing of 27.5 Å, which is consistent with the computed long-axis molecular length of the DTCDI acceptor unit (~32 Å for ~45° alkyl chain tilting), indicating short-range lamellar ordering, which is favorable for efficient in-plane source-to-drain (S→D) charge-transport. The observed interpenetrating fibre-like morphology and ordered lamellar microstructure of P1 thin-films is consistent with the observed high charge-carrier mobilities, whereas the absence of any microstructural ordering in P3 thin-films results in inferior OTFT performances. Since both P1 and P3 have the same DTCDI acceptor building block, the observed differences in thin-film crystallization could be attributed to the nature of the co-monomer present in the polymeric backbones (unsubstituted monothiophene (P1) *vs.* head-to-head dialkoxybithiophene (P3)), which results in different alky chain densities and different short-/long-range intra/intermolecular interactions.

In conclusion, we have synthesized and characterized a new class of D-A conjugated polymers based on dithienocoronenediimide core. Solution-processed ambipolar OTFTs have been demonstrated with these polymers, and high OTFT charge carrier mobilities up to 0.30 $cm^2 V^{-1} s^{-1}$ and 0.04 $cm^2 V^{-1} s^{-1}$ have been obtained in ambient for electrons and holes, respectively. To the best of our knowledge, these values are the highest reported to date in ambient for an ambipolar polymer in a top-gate/bottom-contact architecture. Furthermore, the current polymers are the first examples of high-performance OTFT semiconductors reported in the coronenediimide family. Undoubtedly, our results show that through rational design and synthesis, π-conjugated diimide-based building blocks remain to be one of the most promising classes of materials for efficient electron/hole charge transport.

Experimental Section

Synthesis of P1: The reagents 2,5-Bis(trimethylstannyl)thiophene (30.2 mg, 0.074 mmol), 5 (100 mg, 0.074 mmol), $Pd_2(dba)_3$ (2.7 mg,

0.0029 mmol), and P(*o*-tolyl)$_3$ (3.6 mg, 0.012 mmol) in anhydrous chlorobenzene (20 mL) were heated at 135 °C for 20 h under nitrogen in a sealed flask. After cooling to room temperature, the dark green viscous reaction mixture was poured into methanol (100 mL). After stirring for 2 h, the precipitated dark solid was collected by gravity filtration. The polymer was subjected to sequential Soxhlet extraction with methanol, acetone, hexanes and chloroform. Finally, the chloroform solution (10 mL) was precipitated into methanol (100 mL). The extraction/precipitation procedure was repeated one more time. The final precipitated polymer was collected by vacuum filtration and dried in a vacuum oven (60 °C, overnight) to afford the pure polymer as a dark solid (80 mg, 85% yield). Anal. calcd for $C_{82}H_{102}N_2O_4S_3$: C 77.19, H 8.06, N 2.20; found: C 76.97, H 8.06, N 2.37; GPC (RT in THF): M_n = 10,753 g mol^{-1}, M_w = 17,312 g mol^{-1}, and PDI = 1.61 (against PS standard).

Synthesis of P3: The reagents 5,5′-bis(trimethylstannyl)-3,3′-didodecyloxy-2,2′-bithiophene (135.6 mg, 0.157 mmol), 5 (212.5 mg, 0.157 mmol), $Pd_2(dba)_3$ (5.7 mg, 0.006 mmol), and P(*o*-tolyl)$_3$ (7.6 mg, 0.025 mmol) in anhydrous chlorobenzene (40 mL) were heated at 135 °C for 18 h under nitrogen in a sealed flask. After cooling to room temperature, the dark red viscous reaction mixture was poured into methanol (100 mL). After stirring for 2 h, the precipitated dark solid was collected by gravity filtration. The polymer was subjected to sequential Soxhlet extraction with methanol, acetone, hexanes, and chloroform. Finally, the chloroform solution (10 mL) was precipitated into methanol (120 mL). The extraction/precipitation procedure was repeated one more time. The final precipitated polymer was collected by vacuum filtration and dried in a vacuum oven (60 °C, overnight) to afford the pure polymer as a dark solid (250 mg, 97% yield). Anal. calcd for $C_{104}H_{140}N_2O_6S_4$: C 76.05, H 8.59, N 1.71; found: C 75.75, H 8.37, N 1.71; GPC (RT in THF): M_n = 51,025 g mol^{-1}, M_w 87,252 g mol^{-1}, and PDI = 1.71 (against PS standard).

Fabrication and Characterization of TFT Devices: All processes, except metal evaporation and drying steps, were performed in ambient conditions in a conventional chemistry hood. Top-gate bottom-contact TFTs were fabricated on glass (PGO glass or other sources). Au source-drain contacts (30 nm) were deposited by thermal evaporation to yield channel lengths and widths of 25–75 μm and 0.5–1.5 mm, respectively (W/L = 20). The semiconductor layer is deposited by spin-coating (concentration ~5–10 mg mL^{-1} in DCB, 1500-2000 rpm). Typical semiconductor film thicknesses are ~40-50 nm. Next, the dielectric layer (~500 nm) is spin-coated from polymer solutions (PMMA, ~60–80 mg mL^{-1} in n-BuOAc, 1000–2000 rpm). The semiconductor and the dielectric films were dried at 110 °C overnight in a vacuum oven (<5 mTorr). The devices were completed by thermal evaporation of patterned Au gate contacts (~30 nm thick) through a shadow mask. A Keithley 4200 semiconductor characterization system was used to perform all electrical/TFT characterizations of the top-gate devices. The capacitance of the dielectric film (3.8 nF/cm^2) was measured using GLK Model 3000 digital capacitance meter. The 4200 SCS system consists of three source measurement units, all of which are supplied with remote pre-amplifiers. The other major component of the test system is a Signatone probe station. Triax cable and probes were used for all electrodes to provide the first level of shielding. A dark/metal box enclosure was used to avoid light exposure and to further reduce enviromental noise. The dark box had a triax cable feedthrough panel to maintain consistent triax shielding all the way from the preamps to the end of triax probe tips. Thin Film XRD characterization was performed using a Rigaku ATXG thin film diffractometer with Ni-filtered Cu Kα radiation. AFM images were taken from a JEOL-SPM5200 with a Si cantilever. Film thickness was determined by profilometry using a Veeco Dektak 150.

Supporting Information

Supporting Information is available from the Wiley Online Library or from the author. It includes synthetic procedures and characterizations of compounds 2-5, and T-DTCDI-T, Scheme S1, and Figures S1-S3.

Acknowledgements

We thank Dr. Jangdae Youn for his help with AFM and XRD characterizations.

Received: March 10, 2012
Published online: June 12, 2012

[1] a) A. Facchetti, *Mater. Today.* **2007**, *10*, 28; b) P. M. Beaujuge, J. M. J. Fréchet, *J. Am. Chem. Soc.* **2011**, *133*, 20009; c) X. Zhao, X. Zhan*Chem. Soc. Rev.* **2011**, *40*, 3728; d) K. Mullen, G. Wegner, *Electronic Materials: The Material Approach*, Wiley-VCH, Weinheim, Germany**1998**; e) *Organic Electronics: Materials, Manufacturing, and Applications* (Ed: H. Klauk), Wiley-VCH, Weinheim, Germany **2006**; f) S. S. Lee, M. A. Loth, J. E. Anthony, Y.-L. Loo, *J. Am. Chem. Soc.* **2012**, *134*, 5436; g) K.-J. Baeg, J. Kim, D. Khim, M. Caironi, D.-Y. Kim, I.-K. You, J. R. Quinn, A. Facchetti, Y.-Y. Noh, *ACS Appl. Mater. Interfaces* **2011**, *3*, 3205; h) A. C. Arias, J. D. MacKenzie, I. McCulloch, J. Rivnay, A. Salleo, *Chem. Rev.* **2010**, *110*, 3.

[2] a) A. J. Heeger, *Chem. Soc. Rev.* **2010**, *39*, 2354; b) A. Facchetti, *Chem. Mater.* **2011**, *23*, 733; c) M. L. Chabinyc, Y.-L. Loo, *J. Macromol. Sci. Polymer Rev.* **2006**, *46*, 1; d) Y. Li, P. Sonar, S. P. Singh, M. S. Soh, M. van Meurs, J. Tan, *J. Am. Chem. Soc.* **2011**, *133*, 2198; e) S. S. Lee, C. S. Kim, E. D. Gomez, B. Purushothaman, M. F. Toney, C. Wang, A. Hexemer, J. E. Anthony, Y.-L. Loo, *Adv. Mater.* **2009**, *35*, 3605; f) K.-J. Baeg, D. Khim, J.-H. Kim, M. Kang, I.-K. You, D.-Y. Kim, Y.-Y. Noh, *Org. Electron.* **2011**, *12*, 634; g) J. Soeda, Y. Hirose, M. Yamagishi, A. Nakao, T. Uemura, K. Nakayama, M. Uno, Y. Nakazawa, K. Takimiya, J. Takeya, *Adv. Mater.* **2011**, *23*, 3309; h) K.-J. Baeg, Y.-Y. Noh, J. Ghim, S.-J. Kang, H. Lee, D.-Y. Kim, *Adv. Mater.* **2006**, *18*, 3179; i) C. Piliego, D. Jarzab, G. Gigli, Z. Chen, A. Facchetti, M. A. Loi, *Adv. Mater.* **2009**, *21*, 1573; j) C. Kim, P.-Y. Huang, J.-W. Jhuang, M.-C. Chen, J.-C. Ho, T.-S. Hu, J.-Y. Yan, L.-H. Chen, G.-H. Lee, A. Facchetti, T. J. Marks, *Org. Electron.* **2010**, *11*, 1363; k) C. Kim, M-C. Chen, Y.-J. Chiang, Y.-J. Guo, J. Youn, H. Huang, Y.-J. Liang, Y.-J. Lin, Y.-W. Huang, T.-S. Hu, G.-H. Lee, A. Facchetti, T. J. Marks, *Org. Electron.* **2010**, *11*, 801.

[3] a) A. Tsumura, H. Koezuka, T. Ando, *Appl. Phys. Lett.* **1986**, *49*, 1210; b) C. Wang, H. Dong, W. Hu, Y. Liu, D. Zhu, *Chem. Rev.* **2012**, *112*, 2208; c) M. L. Chabinyc, A. Salleo, *Chem. Mater.* **2004**, *16*, 4509; d) M. Melucci, M. Zambianchi, L. Favaretto, M. Gazzano, A. Zanelli, M. Monari, R. Capelli, S. Troisi, S. Toffanin, M. Muccini, *Chem. Commun.* **2011**, *47*, 11840; e) G. Generali, F. Dinelli, R. Capelli, S. Toffanin, M. Muccini, *J. Phys. D: Appl. Phys.* **2011**, *44*, 224018; f) C. H. Peters, I. T. Sachs-Quintana, W. R. Mateker, T. Heumueller, J. Rivnay, R. Noriega, Z. M. Beiley, E. T. Hoke, A. Salleo, M. D. McGehee, *Adv. Mater.* **2012**, *24*, 663; g) J. Dacuna, A. Salleo, *Phys. Rev. B* **2011**, *84*, 195209; h) A. Salleo, R. J. Kline, D. M. DeLongchamp, M. L. Chabinyc, *Adv. Mater.* **2010**, *22*, 3812; i) J. Rivnay, M. F. Toney, Y. Zheng, I. V. Kauvar, Z. Chen, V. Wagner, A. Facchetti, A. Salleo, *Adv. Mater.* **2010**, *22*, 4359.

[4] H. Yan, Z. Chen, Y. Zheng, C. Newman, J. R. Quinn, F. Dötz, M. Kastler, A. Facchetti, *Nature* **2009**, *457*, 679.

[5] a) I. McCulloch, M. Heeney, C. Bailey, K. Genevicius, I. MacDonald, M. Shkunov, D. Sparrowe, S. Tierney, R. Wagner, W. Zhang, M. L. Chabinyc, R. J. Kline, M. D. McGehee, M. F. Toney, *Nat. Mater.* **2006**, *5*, 328; b) I. Osaka, T. Abe, S. Shinamura, E. Miyazaki, K. Takimiya, *J. Am. Chem. Soc.* **2010**, *132*, 5000; c) J. Mei, D. H. Kim, A. L. Ayzner, M. F. Toney, Z. Bao, *J. Am. Chem. Soc.* **2011**, *133*, 20130; d) X. Guo, F. S. Kim, S. A. Jenekhe, M. D. Watson, *J. Am. Chem. Soc.* **2009**, *131*, 7206; e) M. Zhang, H. N. Tsao, W. Pisula, C. Yang, A. K. Mishra, K. Müllen, *J. Am. Chem. Soc.* **2007**, *129*, 3472.

[6] a) H. Zhou, L. Yang, A. C. Stuart, S. C. Price, S. Liu, W. You, *Angew. Chem. Int. Ed.* **2011**, *50*, 2995; b) E. Zhou, J. Cong, Q. Wei, K. Tajima, C. Yang, K. Hashimoto, *Angew. Chem. Int. Ed.* **2011**, *50*, 2799; c) H. J. Son, W. Wang, T. Xu, Y. Liang, Y.Wu, G. Li, L. Yu, *J. Am. Chem. Soc.* **2011**, *133*, 1885; d) C. Piliego, M. A. Loi, *J. Mater. Chem.* **2012**, *22*, 4141.

[7] a) L. Bürgi, M. Turbiez, R. Pfeiffer, F. Bienewald, H.-J. Kirner, C. Winnewisser, *Adv. Mater.* **2008**, *20*, 2217; b) T. Dallos, D. Beckmann, G. Brunklaus, M.Baumgarten, *J. Am. Chem. Soc.* **2011**, *133*, 13898; c) J. D. Yuen, R. Kumar, D. Zakhidov, J. Seifter, B. Lim, A. J. Heeger, F. Wudl, *Adv. Mater.* **2011**, *23*, 3780; d) J. C. Bijleveld, A. P. Zoombelt, S. G. J. Mathijssen, M. M. Wienk, M. Turbiez, D. M. de Leeuw, R. A. J. Janssen, *J. Am. Chem. Soc.* **2009**, *131*, 16616; e) M. Shahid, T. McCarthy-Ward, J. Labram, S. Rossbauer, E. B. Domingo, S. E. Watkins, N. Stingelin, T. D. Anthopoulos, M. Heeney, *Chem. Sci.* **2012**, *3*, 181.

[8] a) Z. Chen, M. J. Lee, R. Shahid Ashraf, Y. Gu, S. Albert-Seifried, M. M. Nielsen, B. Schroeder, T. D. Anthopoulos, M. Heeney, I. McCulloch, H. Sirringhaus, *Adv. Mater.* **2012**, *24*, 647; b) P. Sonar, S. P. Singh, Y. Li, M. S. Soh, A. Dodabalapur, *Adv. Mater.* **2010**, *22*, 5409; c) A. R. Mohebbi, J. Yuen, J. Fan, C. Munoz, M. F. Wang, R. S. Shirazi, J. Seifter, F. Wudl, *Adv. Mater.* **2011**, *23*, 4644.

[9] a) H. Usta, C. Risko, Z. Wang, H. Huang, M. K. Deliomeroglu, A. Zhukhovitskiy, A. Facchetti, T. J. Marks, *J. Am. Chem. Soc.* **2009**, *131*, 5586; b) M. Irimia-Vladu, E. D. Glowacki, P. A. Troshin, G. Schwabegger, L. Leonat, D. K. Susarova, O. Krystal, M. Ullah, Y. Kanbur, M. A. Bodea, V. F. Razumov, H. Sitter, S. Bauer, N. S. Sariciftci, *Adv. Mater.* **2012**, *24*, 375.

[10] a) R. P. Ortiz, H. Herrera, C. Seoane, J. L.Segura, A. Facchetti, T. J. Marks, *Chem. Eur. J.* **2012**, *18*, 532; b) N. A. Minder, S. Ono, Z. Chen, A. Facchetti, A. F. Morpurgo, *Adv. Mater.* **2012**, *24*, 503.

[11] H. Usta, A. Facchetti, T. J. Marks, *Acc. Chem. Res.* **2011**, *44*, 501.

[12] a) F. S. Kim, X. Guo, M. D. Watson, S. A. Jenekhe, *Adv. Mater.* **2010**, *22*, 478; b) C. Huang, S. Barlow, S. R. Marder, *J. Org. Chem.* **2011**, *76*, 2386; c) X. Zhan, A. Facchetti, S. Barlow, T. J. Marks, M. A. Ratner, M. R. Wasielewski, S. R. Marder, *Adv. Mater.* **2011**, *23*, 268.

[13] a) S. Alibert-Fouet, I. Seguy, J.-F. Bobo, P. Destruel, H. Bock, *Chem. Eur. J.* **2007**, *13*, 1746; b) C. L. Eversloh, C. Li, K. Müllen, *Org. Lett.* **2011**, *13*, 4148.

[14] a) Z. An, J. Yu, B. Domercq, S. C. Jones, S. Barlow, B. Kippelen, S. R. Marder, *J. Mater. Chem.* **2009**, *19*, 6688; b) F. Nolde, W. Pisula, S. Müller, C. Kohl, K. Müllen, *Chem. Mater.* **2006**, *18*, 3715; c) U. Rohr, C. Kohl, K. Mullen, A. van de Craats, J. Warman, *J. Mater. Chem.* **2001**, *11*, 1789.

[15] While our studies were underway, a dithienocoronenediimide-based small molecule was reported as a donor unit in BHJ-OPVs with a power conversion efficiency of 1.42%. H. Choi, S. Paek, J. Song, C. Kim, N. Cho, J. Ko, *Chem. Commun.* **2011**, *47*, 5509.

[16] a) B. A. Jones, A. Facchetti, M. R. Wasielewski, T. J. Marks, *J. Am. Chem. Soc.* **2007**, *129*, 15259; b) J. Huang, H. Fu, Y. Wu, S. Chen, F. Shen, X. Zhao, Y. Liu, J. Yao*J. Phys. Chem. C* **2008**, *112*, 2689.

[17] a) T. Okamoto, Y. Jiang, H. A. Becerril, S. Hong, M. L. Senatore, M. L. Tang, M. F. Toney, T. Siegrist, Z. Bao, *J. Mater. Chem.* **2011**, *21*, 7078; b) I. Osaka, R. D. McCullough, *Acc. Chem. Res.* **2008**, *41*, 1202; c) C. Yang, F. P. Orfino, S. Holdcroft, *Macromolecules* **1996**, *29*, 6510; d) K. Kanai, T. Miyazaki, H. Suzuki, M. Inaba, Y. Ouchi, K. Seki, *Phys. Chem. Chem. Phys.* **2010**, *12*, 273.

[18] a) P. Rajasingh, R. Cohen, E. Shirman, L. J. W. Shimon, B. Rybtchinski, *J. Org. Chem.* **2007**, *72*, 5973; b) F. Würthner, V. Stepanenko, Z. Chen, C. R. S. Möller, N. Kocher, D. Stalke, *J. Org. Chem.* **2004**, *69*, 7933; c) R. K. Dubey, A.Efimov, H. Lemmetyinen, *Chem. Mater.* **2011**, *23*, 778.

[19] a) B. A. Jones, M. J. Ahrens, M. H. Yoon, A. Facchetti, T. J. Marks, M. R. Wasielewski, *Angew. Chem. Int. Ed.* **2004**, *43*, 6363; b) X. Zhan, Z. Tan, B. Domercq, Z. An, X. Zhang, S. Barlow, Y. Li, D. Zhu, B. Kippelen, S. R. Marder, *J. Am. Chem. Soc.* **2007**, *129*, 7246.

[20] Z. Chen, Y. Zheng, H. Yan, A. Facchetti, *J. Am. Chem. Soc.* **2009**, *131*, 8.

[21] a) M. Kastler, W. Pisula, D. Wasserfallen, T. Pakula, K. Mullen, *J. Am. Chem. Soc.* **2005**, *127*, 4286; b) J. Wu, A. Fechtenkotter, J. Gauss, M. D. Watson, M. Kastler, C. Fechtenkotter, M. Wagner, K. Mullen, *J. Am. Chem. Soc.* **2004**, *126*, 11311; c) M. D. Watson, F. Jäckel, N. Severin, J. P. Rabe, K. Mullen, *J. Am. Chem. Soc.* **2004**, *126*, 1402.

[22] a) W. W. H. Wong, T. B. Singh, D. Vak, W. Pisula, C. Yan, X. Feng, E. L. Williams, K. L. Chan, Q. Mao, D. J. Jones, C.-Q. Ma, K. Mullen, P. Bauerle, A. B. Holmes, *Adv. Funct. Mater.* **2010**, *20*, 927; b) W. W. H. Wong, C.-Q. Ma, W. Pisula, C. Yan, X. Feng, D. J. Jones, K. Mullen, R. A. J. Janssen, P. Bauerle, A. B. Holmes, *Chem. Mater.* **2010**, *22*, 457.

[23] a) M. Adachi, Y. Nagao, *Chem. Mater.* **2001**, *13*, 662; b) M. Adachi, Y. Murata, *J. Phys. Chem. A* **1998**, *102*, 841.

[24] *Printed Organic and Molecular Electronics*, (Eds: D. Gamota, P. Brazis, K. Kalyanasundaram, J. Zhang), Kluwer Academic Publishers, New York **2004**.